ORIGINAL RESEARCH

Novel Noninvasive Assessment of Pulmonary Arterial Stiffness Using Velocity Transfer Function

Ankur Gupta, MD, PhD; Oleg F. Sharifov, MD, PhD; Steven G. Lloyd, MD, PhD; Jose A. Tallaj, MD; Inmaculada Aban, PhD; Louis J. Dell'italia, MD; Thomas S. Denney Jr, PhD; Himanshu Gupta, MD

***Background*—**Pulmonary artery (PA) stiffness is associated with increased pulmonary vascular resistance (PVR). PA stiffness is accurately described by invasive PA impedance because it considers pulsatile blood flow through elastic PAs. We hypothesized that PA stiffness and impedance could be evaluated noninvasively by PA velocity transfer function (VTF), calculated as a ratio of the frequency spectra of output/input mean velocity profiles in PAs.

***Methods and Results*—**In 20 participants (55±19 years, 14 women) undergoing clinically indicated right-sided heart catheterization, comprehensive phase-contrast and cine-cardiac magnetic resonance imaging was performed to calculate PA VTF, along with right ventricular mass and function. PA impedance was measured as a ratio of frequency spectra of invasive PA pressure and echocardiographically derived PA flow waveforms. Mean PA pressure was 29.5±13.6 mm Hg, and PVR was 3.5±2.8 Wood units. A mixed-effects model showed VTF was significantly associated with PA impedance independent of elevation in pulmonary capillary wedge pressure (P=0.005). The mean of higher frequency moduli of VTF correlated with PVR (ρ=0.63; P=0.003) and discriminated subjects with low (n=10) versus elevated PVR (≥2.5 Wood units, n=10), with an area under the curve of 0.95, similar to discrimination by impedance (area under the curve=0.93). VTF had a strong inverse association with right ventricular ejection fraction (ρ=−0.73; P<0.001) and a significant positive correlation with right ventricular mass index (ρ=0.51; P=0.02).

***Conclusions*—**VTF, a novel right ventricular–PA axis coupling parameter, is a surrogate for PA impedance with the potential to assess PA stiffness and elevation in PVR noninvasively and reliably using cardiac magnetic resonance imaging. **(*J Am Heart Assoc.* 2018;7:e009459. DOI: 10.1161/JAHA.118.009459.)**

Key Words: cardiac magnetic resonance imaging • pulmonary artery impedance • pulmonary artery stiffness • pulmonary vascular resistance • velocity transfer function

Pulmonary arterial hypertension (PAH) is defined on the basis of the elevated pulmonary artery (PA) pressures and/or pulmonary vascular resistance (PVR).[1] PVR, a ratio of mean pressure gradient and blood flow in PA, assumes nonelastic PA conduits with static and nonpulsatile pressure-volume relationship.[2] However, PAs are highly distensible, with pulsatile energy losses in pulmonary circulation 2.5 times greater than that in systemic circulation.[3–5] Pulmonary impedance, the relationship of pulsatile pressure with pulsatile flow in frequency domain, is thus a more accurate measure of afterload in pulmonary circulation compared with PVR.[3–5] Its modulus (magnitude) has the same units as PVR but, in addition, it also accounts for the viscoelastic properties of the vessel (vessel stiffness or compliance) as well as pulse wave reflections.[4–6] Determinants of pulmonary impedance and PA pressure and flow, in turn, are closely coupled to right ventricular (RV) geometry, function, and chamber pressures.[7]

It has been shown that PA stiffness increases early during PAH when PAH is detectable only with exercise before overt pressure elevations occur at rest.[8] Thus, decrease in PA compliance and increase in PA stiffness represent the earliest physiological manifestation of PA remodeling. This results in increased RV afterload, as measured by PA impedance.[5]

From the Division of Cardiovascular Disease, Departments of Medicine (A.G., O.F.S., S.G.L., J.A.T., L.J.D., H.G.) and Biostatistics (I.A.), University of Alabama at Birmingham, AL; Division of Cardiovascular Medicine and Department of Radiology, Brigham and Women's Hospital Heart and Vascular Center, Harvard Medical School, Boston, MA (A.G.); Veterans Affairs Medical Center, Birmingham, AL (S.G.L., J.A.T., L.J.D., H.G.); Department of Electrical and Computer Engineering, Auburn University, Auburn, AL (T.S.D.); and Valley Medical Group, Ridgewood, NJ (H.G).

Accompanying Data S1, Tables S1 through S4, and Figures S1 through S7 are available at https://www.ahajournals.org/doi/suppl/10.1161/JAHA.118.009459

Correspondence to: Himanshu Gupta, MD, 970 Linwood Ave, Ste 102, Paramus, NJ 07652. E-mail: gupthi@valleyhealth.com

Received April 12, 2018; accepted July 31, 2018.

Clinical Perspective

What Is New?

- We have introduced a novel noninvasive parameter of right ventricular–pulmonary artery (PA) coupling, PA velocity transfer function, calculated as a ratio of the frequency spectra of output/input mean velocity profiles in the pulmonary arteries.
- Velocity transfer function has a strong association with invasive PA impedance independent of elevation in pulmonary capillary wedge pressure and accurately assesses PA stiffness and elevation in pulmonary vascular resistance.

What Are the Clinical Implications?

- We have demonstrated a novel rapid noninvasive method using phase-contrast cardiac magnetic resonance imaging that reliably estimates PA stiffness and pulmonary vascular resistance and can be used as a surrogate of invasive PA impedance.
- After prospective validation in larger and longitudinal studies, this proposed method could be used for noninvasive screening of pulmonary hypertension and follow-up assessment of PA stiffness in clinical studies.

Although pulmonary impedance measurements are feasible,[9] the need for invasive PA catheterization and simultaneous registration of PA flow (either invasively or by echocardiography) limits its clinical use. PA compliance and stiffness can be currently measured on the basis of the ratio of change in luminal diameter of PA with cardiac cycle (measured on echocardiography or cardiac magnetic resonance [CMR] imaging) and change in pressure (measured invasively). However, the need for invasive pressure measurements limits its use for detection of early PA remodeling or serial measurements. Pulse wave velocity (PWV) has been described as a noninvasive measure of arterial stiffness.[6] However, it has not been adopted for clinical use because of difficulty in reliably measuring PWV, its dependence on hemodynamic conditions, and need for a high temporal resolution CMR.

Herein, we propose a novel completely noninvasive CMR-derived measure of PA stiffness, velocity transfer function (VTF). This novel parameter relies on the fact that the compliance of the PA causes frequency-dependent changes in the shape of input velocity profile as it travels through the artery, thereby producing the output velocity profile. The stiffer the PA, the lower the change in velocity profile from input to output. A compliant PA leads to dampening of magnitude and change in shape of velocity waveform as the blood traverses through it. The frequency-dependent relationship between the input and output velocity profiles can be described by a transfer function, which is the ratio between the frequency spectra of output/input velocity. Details on the rationale for VTF are presented in Data S1, Figures S1 and S2. We hypothesized that stiff and elastic PA can be differentiated on the basis of the performance of VTF harmonics, consistent with performance of impedance harmonics. In this work, we sought to prospectively validate this hypothesis for pulmonary circulation using directly measured pulmonary impedance as a reference standard.

Methods

Sample Population and Study Design

The data, analytic methods, and study materials will not be made available to other researchers for purposes of reproducing the results or replicating the procedure. Subjects with clinically indicated outpatient right-sided heart catheterization (RHC) and willing to undergo CMR were prospectively recruited at the University of Alabama at Birmingham Hospital and The Kirklin Clinic. Subjects were excluded from the study if they were receiving inotropic therapy or ventricular assist device, had a history of heart or lung transplantation, or had any contraindication for CMR. A total of 104 subjects were screened, of which 39 were eligible to participate in the study. Twenty-six subjects consented to participate, of which 6 unsuccessfully attempted CMR examination because of realization of previously unknown claustrophobia. No medications were given for claustrophobia to avoid altering hemodynamic state at the time of CMR. A total of 20 participants were, thus, enrolled: 10 cases with moderately to severely elevated PVR (>2.5 Wood units [WUs]) and 10 controls with normal or mildly elevated resting PVR (<2.5 WUs).[10,11] The study was approved by the University of Alabama at Birmingham Institutional Review Board.

RHC, Doppler Echocardiography, and Invasive Impedance Measurement

After informed consent, participants underwent clinically indicated RHC with 5F Swan-Ganz fluid-filled catheter via right internal jugular vein under local anesthesia only without intravenous sedation. PA pressure waveform was then recorded in main PA 0.5 to 1 cm distal to pulmonic valve. With study subject in left lateral decubitus position and ultrasound transducer in left parasternal intercostal space (usually third or fourth), short-axis view of heart was obtained at the level of the aortic valve. Pulsed-wave Doppler echocardiography was then obtained in this view with 2-mm sample volume placed 0.5 to 1 cm distal to pulmonic valve in the main PA. Doppler echocardiography was obtained using Philips IE33 ultrasound system. Acquisition of RHC and Doppler echocardiography was done either simultaneously or

immediately after the first modality (mean time difference between the 2 modalities was 2±3 minutes). Bland-Altman analysis revealed excellent correlation and agreement between intermodality heart rate (Table S1). PA pressure obtained from invasive RHC and PA blood flow velocity profiles obtained from pulsed-wave Doppler were synchronized using ECG artifact, as described before.[12] These waveforms were then digitized (Figure S3) using WebPlotDigitizer, version 3.8. The digital data were extracted as comma separated values format. The velocity profile was converted to flow profile using the formula: Q(t)=(cardiac output on RHC/mean velocity)×V(t), where Q(t) is the calculated flow-time history and V(t) is the velocity-time history obtained from digitized pulsed wave Doppler waveform.[12] Impedance was then calculated by obtaining discrete Fourier transformation on the digitized data using Matlab, version 2015a. PVR was determined as follows: PVR=(PA mean pressure−pulmonary capillary wedge pressure)/cardiac output. Other parameters of PA stiffness, including PA/aortic diameter ratio, pulsatility, compliance, capacitance, distensibility, elasticity, and stiffness index, were also measured. The definitions of PA stiffness parameters are detailed in Table S2.

CMR and VTF Measurement

Comprehensive CMR consisting of cine and phase contrast sequences was performed on the same day of pressure-flow measurements to maintain the close temporal relationship and to minimize significant alteration in hemodynamic state (mean time difference between RHC and CMR was 2.4±1.2 hours). Patient had no medications or interventions in between pressure-flow measurements on RHC and VTF measurement on CMR. Bland-Altman analysis revealed excellent correlation and agreement between intermodality heart rate, blood pressure, and cardiac index (Table S1).

CMR was performed on a 1.5-T magnetic resonance scanner (GE Signa, Milwaukee, WI) optimized for cardiac application. Phase-contrast CMR technique was used for flow measurements in the right PA, the longest branch of the pulmonary trunk that courses perpendicularly away from the pulmonary trunk before further segmentation. The proximal plane was positioned en face to the right PA 2 cm after its origin from the main PA. The distal plane was positioned parallel to the proximal plane ≈5 cm (4.9±2.1 cm) distal to it. VTF was computed between measured mean velocity profiles at the proximal (input) and distal (output) portion of the right PA by taking the Fourier transform of the velocity profile at each location and dividing one by other at each harmonic as follows: $VTF=V_{output}(f)/V_{input}(f)$, where V_{output} is velocity profile at distal right PA and V_{input} is velocity profile at proximal right PA. Further details on the rationale for VTF and its calculation are presented in Data S1, Figures S1 and S2. Phase-contrast CMR was performed using electrocardiographically gated, breath-hold fast gradient recalled echo phase-contrast sequence. Typical parameters were as follows: field of view, 40 cm; scan matrix, 256×128; encoding velocity, 150 cm/s; number of excitations, 1; flip angle, 15°; repetition/echo times, 7.8/3.2 ms; band width, ±31.25 kHz; 8 views per segment. The spatial resolution was 1.5625×1.5625 mm in-plane, 8-mm thick slices. Twenty phases were reconstructed. Parameters of phase-contrast CMR were consistent with published guidelines.[13,14] Contours were drawn, and mean velocity-time profiles over a cardiac cycle were computed using CAAS MR Flow 1.2 (Pie Medical Imaging, the Netherlands) and exported to MATLAB 2015a for VTF computation (Figure S4).

CMR and Assessment of RV Function, Remodeling, and RV-PA Coupling

RV systolic function and remodeling were assessed by cine-CMR derived RV ejection fraction, RV stroke volume index, RV mass index (RVMI), RV end-diastolic volume index, all indexed to body surface area, and RV mass/RV end-diastolic volume ratio. For assessment of these parameters, an electrographically gated breath-hold steady-state free-precision technique was used to obtain standard 2-chamber, 4-chamber, and short-axis views with following general parameters: prospective electrocardiographic gating; slice thickness, 8 mm; 2-mm interslice gap; field of view, 40×40 cm; scan matrix, 224×128; flip angle, 45°; repetition/echo times, 3.8/1.6 ms. Twenty cardiac phases were reconstructed with 8 views per segment. Short-axis stack was positioned from an end-diastolic 4-chamber image, centered parallel to the mitral annulus and perpendicular to the septum, starting 1 cm proximal to the mitral valve to 1 cm beyond the apex. Analysis was performed using CAAS MRV 3.4 (Pie Medical Imaging, the Netherlands). Assessments of ventricular mass, volumes, and function were then obtained, as previously described.[15,16] RV-PA coupling was assessed by a ratio of RV end-systolic elastance (Ees)/arterial elastance (Ea) that was estimated by "volume" method (Ees/Ea=RV stroke volume/end systolic volume).[17,18] Although the volume method underestimates Ees/Ea, it strongly correlates to Ees/Ea and appears to be a better predictor of PAH outcome.[18,19] Ees was estimated as RV end systolic pressure/end systolic volume, and Ea was estimated as RV end systolic pressure/stroke volume.[17–21] One patient completed only phase-contrast portion of CMR and did not complete cine CMR because of claustrophobia. This patient was retained in analysis of VTF (calculated from phase-contrast CMR) but excluded from RV structure and function analysis.

Statistical Analyses

All data were presented as the mean±SD for normally distributed variables and median (interquartile range) for nonnormally distributed variables. Study participants were divided into 2 groups. One group consisted of participants with normal or mildly elevated resting PVR (low PVR group; <2.5 WUs).[10,11] The other group included participants with moderately to severely elevated PVR (high PVR group; ≥2.5 WUs).[11] Demographic, clinical, hemodynamic, and imaging characteristics of these PVR groups were compared using *t* test or Mann-Whitney test as appropriate for continuous variables and Fisher's exact test for categorical variables.

Repeated mixed-model analysis was performed on 0 and first 7 harmonics of impedance as dependent variable and VTF as predictor variable to assess linear association of VTF with impedance. Unstructured covariance structure for the error term was fitted to accommodate correlation between various harmonics from the same subject.

Zero harmonic represents the ratio of mean values. As the impedance is a ratio of pressure and flow waveforms, 0 harmonic represents ratio of mean pressure and mean flow, which approximates PVR. The effect of stiffness is often best observed in modulus of first 2 harmonics of impedance, with stiffer artery leading to high 0 harmonic modulus and delay in decline of modulus with high moduli in early harmonics. We, therefore, averaged the 0 and first 2 harmonics of impedance to form the mean low-frequency modulus (MLFM) of impedance. However, for VTF, 0 harmonic represents ratio of 2 mean velocities (input and output) and is close to 1. VTF modulus remains close to 1 at earlier harmonics, and differentiation between VTF moduli with varying degree of impedance is expected to happen at higher harmonics. We, therefore, averaged fifth, sixth, and seventh harmonics for the VTF to form the mean high-frequency modulus (MHFM) of VTF. The strength of association between impedance (MLFM), VTF (MHFM), PVR, and RV remodeling was studied using Spearman's rank correlation coefficient (ρ).

To estimate intraobserver and interobserver reliability in the calculation of VTF, phase-contrast CMR studies were evaluated by 2 cardiologists (twice by A.G. and once by H.G.) in an independent and blinded manner. Intraclass correlation was used to investigate intraobserver and interobserver reliability in calculation of MHFM of VTF, as previously described,[22] using openly available SAS code (https://www.hsph.harvard.edu/donna-spiegelman/software/icc9/). Relative bias, defined as mean paired difference in MHFM of VTF, was used to investigate intraobserver and interobserver agreement.

Receiver operating characteristic curve analysis was performed to identify the optimal thresholds of the impedance MLFM and VTF MHFM for predicting PVR at predefined values. The following PVR thresholds were tested: ≥1.6 WUs (traditional normal range upper limit)[23,24]; ≥2.0 WUs (age-related normal values upper limit)[10,25]; ≥2.5 WUs (moderately to severe PVR increase associated with increased PA stiffness)[11,26]; ≥3.0 WUs (recommended cutoff for PAH diagnosis).[1,25] A 95% confidence interval (CI) for area under the curve (AUC) of the receiver operating characteristic curve and the *P* value to test the null hypothesis that AUC=0.5 by nonparametric methods were calculated. The Youden index criterion was used to identify the best cutoff value from the receiver operating characteristic curve. All analyses were performed using SAS, 9.4 (SAS Institute Inc, Cary, NC), or SPSS, version 23 (IBM, Armonk, NY). *P*<0.05 was considered statistically significant.

Results

Clinical, Hemodynamic, and Imaging Characteristics

A total of 20 participants were enrolled, with a mean age of 55 years; 14 (70%) were women, and 17 (85%) were white (Table 1). Average PVR, PA mean pressure, and pulmonary capillary wedge pressure were 3.5±2.8 WUs, 29.5±13.6 mm Hg, and 12.3±6.6 mm Hg, respectively. Figure 1 further characterizes participants with low PVR (<2.5 WUs; average PVR, 1.3±0.6 WUs; n=10) and those with high PVR (≥2.5 WUs; average PVR, 5.6±2.6 WUs; n=10) with respect to the presence and type of pulmonary hypertension. The causes of PAH in patients with elevated PVR and elevated mean pulmonary artery pressure (n=8) were idiopathic (n=4), interstitial lung disease (n=1), connective tissue disease (n=1), chronic thromboembolic pulmonary hypertension (n=1), and amyloidosis (n=1), with a median time from diagnosis of 38 months (range, 8–115 months). In patients with elevated PVR (2.5–3 WUs) and normal mean pulmonary artery pressure (n=2), the underlying cause was interstitial lung disease in both patients, with time from diagnosis of 5 and 90 months, respectively. There were higher PA systolic, diastolic, mean, and pulse pressures and lower cardiac index in the high PVR group compared with the low PVR group (Table 2). CMR-derived RVMI, end-diastolic volume index, and mass/volume ratio were also higher in elevated PVR group, whereas left ventricular characteristics were similar in both groups (Table 2). Ees/Ea ratio as an estimate of RV-PA coupling was lower in the high PVR group compared with low PVR group (1.2±0.5 versus 2.0±0.9; *P*<0.01). Although Ees was not significantly different between groups, Ea was higher in the high PVR group (Table 2).

Table 1. Demographics and Clinical Characteristics

Clinical Characteristics	All (n=20)	Low PVR (<2.5 WUs) (n=10)	High PVR (≥2.5 WUs) (n=10)
Age, y	55±19	51±21	60±15
Female sex	14	9	5
Race			
Black	3	2	1
White	17	8	9
Body mass index, kg/m^2	27.6±6.9	28.2±7.5	26.9±6.6
Obesity	7	4	3
Smoking			
Never	11	7	4
Past	9	3	6
Current	0	0	0
Diabetes mellitus	2	2	0
Hypertension	9	5	4
Dyslipidemia	11	5	6
Coronary artery disease	3	2	1
Congestive heart failure	4	2	2
COPD	1	1	0
Interstitial lung disease	4	1	3
Obstructive sleep apnea	4	2	2
New York Heart Association class			
1	2	2	0
2	10	4	6
3	8	4	4
Chronic kidney disease (eGFR <60 mL/min)	5	3	2
Medications			
Oral nitrates	2	1	1
Phosphodiesterase inhibitors	7	2	5
Endothelin receptor antagonists	3	1	2
Prostacyclin analogues	2	0	2
Calcium channel blockers	6	4	2
β Blockers	7	5	2
ACEIs/ARBs	3	2	1
Aldosterone antagonists	6	3	3

Continuous variables are given as mean±SD, and discrete variables are given as number of individuals. ACEI indicates angiotensin-converting enzyme inhibitor; ARB, angiotensin receptor blocker; COPD, chronic obstructive pulmonary disease; eGFR, estimated glomerular filtration rate; PVR, pulmonary vascular resistance; WU, Wood unit.

Among the traditional measures of PA stiffness, the completely noninvasive measures (PA/aortic diameter ratio and pulsatility) were not significantly different among the groups with high or low PVR. The invasive parameters of PA stiffness that require both RHC and dynamic imaging of PA showed lower compliance, capacitance, and distensibility of PA and higher elastic modulus in the high PVR group compared with low PVR group (Table 3).

Association of VTF With Impedance

Mixed-model analysis showed a significant linear association of VTF with impedance (P=0.01). The association between VTF and impedance remained significant after adjustment for elevation in pulmonary capillary wedge pressure (P=0.005). There was also a significant correlation between MHFM of VTF and MLFM of impedance (Spearman's ρ=0.49; 95% CI, 0.41–0.77; P=0.03; see Figure S5A).

Association of VTF and Invasive Impedance With PVR

Figure 2A and 2B shows VTF and impedance averaged by groups with low or high PVR. The MHFM of VTF as well as MLFM of impedance were significantly different in the 2 groups (P<0.001 for both comparisons; Table 3). There was significant correlation between MHFM of VTF and PVR (Spearman's ρ=0.63; 95% CI, 0.24–0.84; P=0.003; see Figure S5B) and MLFM of impedance and PVR (Spearman's ρ=0.86; 95% CI, 0.67–0.94; P<0.001; see Figure S5C).

Figure 3 shows receiver operating characteristic curves for impedance and VTF moduli to identify subjects with PVR ≥2.5 WUs. The MHFM of VTF had an AUC of 0.95 (95% CI, 0.86–1.00; P=0.001), comparable with the results obtained for MLFM of impedance (AUC, 0.93; 95% CI, 0.82–1.00; P=0.001). The optimal cutoff point for MHFM of VTF was 1.0, with sensitivity of 90%, specificity of 90%, positive predictive value of 90%, and negative predictive value of 90%. VTF MHFM also demonstrated consistently high AUC values (>0.80) in identifying the subjects with PVR reaching other diagnostic thresholds (1.6, 2, and 3 WUs; Figure S6).

MHFM of VTF showed significant moderate correlation with other parameters of pulmonary arterial stiffness, including pulsatility, compliance, capacitance, distensibility, and elastic modulus (Table S3).

Association of VTF With RV Structure, Function, and RV-PA Coupling

MHFM of VTF showed significant positive correlation with RVMI (Spearman's ρ=0.51; P=0.02) and strong negative correlation with RV ejection fraction (Spearman's

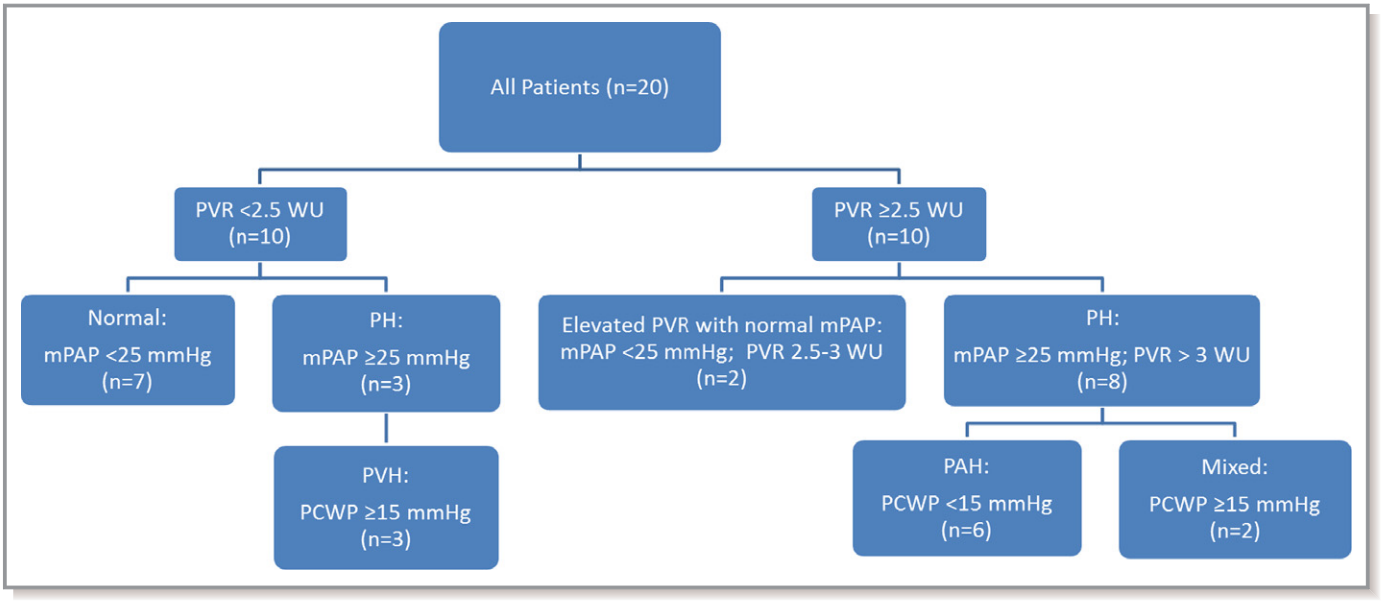

Figure 1. Study participant distribution based on pulmonary vascular resistance (PVR) and/or pulmonary artery pressures. mPAP indicates mean pulmonary artery pressure; PCWP, pulmonary capillary wedge pressure; PH, pulmonary hypertension; PVH, pulmonary venous hypertension; WU, Wood unit.

ρ=−0.73; P<0.001). The RV end-diastolic volume index and RV mass/end-diastolic volume ratio tended to be higher and RV stroke volume tended to be lower with increasing PA stiffness, as measured by MHFM of VTF, although these associations were not statistically significant (Table 4). There was a strong negative correlation between MHFM of VTF and Ees/Ea ratio (Spearman's ρ=−0.83; P<0.001). There was also a positive significant correlation between MHFM of VTF and Ea (Spearman's ρ=0.60; P<0.01), whereas the correlation between MHFM of VTF and Ees was negative and not statistically significant (Spearman's ρ=−0.42; P=0.08; Table 4). Scatterplot graphs of relationship between MHFM of VTF and RV structure, function, and RV-PA coupling parameters are shown in Figure S7.

Reliability of VTF Measurement

Intraobserver and interobserver repeated measurements showed high intraclass correlation (0.93 and 0.94, respectively) and low relative bias (0.19 and 0.05, respectively; P>0.05 for both) in the MHFM of VTF, indicating high intraobserver and interobserver reliability in VTF calculation (Table S4).

Individual Patient Examples

Figure 4A through 4D depicts the VTF profiles from 4 individual study participants, 2 with normal PVR (Figure 4A and 4C) and 2 with abnormal PVR (Figure 4B and 4D), across a range of underlying pathological conditions. These examples highlight the increase in moduli of VTF occurs at higher frequencies (harmonics 5–7) in subjects with elevated PVR, irrespective of the elevation in pulmonary capillary wedge pressure.

Discussion

In this study, we proposed and prospectively validated a robust novel noninvasive surrogate estimate of PA impedance using VTF on CMR. We showed, for the first time to our knowledge, that PA impedance can be detected completely noninvasively using VTF as its surrogate. Specifically, we demonstrated the following: (1) VTF can differentiate across a spectrum of PA impedance and can detect subjects with normal PA impedance versus abnormal PA impedance associated with increased PVR and/or advanced PAH; (2) the detection of elevated PA impedance using VTF is independent of elevation in pulmonary capillary wedge pressure; (3) VTF noninvasively evaluated RV-PA coupling with significant association of VTF with Ees/Ea ratio, Ea, RV ejection fraction, and RVMI; (4) VTF was robust in its measurement, with high intraobserver and interobserver agreement on repeated independent measurements of blinded studies. This study demonstrated that VTF is an accurate and reliable noninvasive surrogate of PA impedance and, thus, can potentially be used as a screening tool for precapillary pulmonary hypertension before more expensive or invasive tests are considered.

Table 2. Invasive- and CMR Imaging–Derived Characteristics

Variables	All (n=20)	Low PVR (<2.5 WUs) (n=10)	High PVR (≥2.5 WUs) (n=10)
Invasive measurements			
Right atrial mean pressure, mm Hg	6.6±4.5	5.6±2.7	7.5±5.8
PA systolic pressure, mm Hg	44.9±22.3	30.9±9.6	59±22.7*
PA diastolic pressure, mm Hg	17±9.3	12±5.9	22±9.5†
PA mean pressure, mm Hg	29.5±13.6	21±6.8	37.9±13.7*
PA pulse pressure, mm Hg	27.9±15.1	18.9±6.6	37±15.9*
PCWP, mm Hg	12.3±6.6	12.7±6.9	11.9±6.6
Thermodilution cardiac index, L/min	3.01±0.7	3.32±0.6	2.7±0.7†
Fick cardiac index, L/min	3.02±0.8	3.42±0.8	2.62±0.6†
PVR, WUs	3.5±2.8	1.3±0.6	5.6±2.6‡
SVR, dyn·s/cm^5	1449±462	1258±333	1640±507
CMR measurements			
RV ejection fraction, %	52±12	57±13	48±11
RV stroke volume index, mL/m^2	37±11	36±12	38±12
RV end-diastolic volume index, mL/m^2	73±21	64±12	81±25
RV mass index, g/m^2	19.2 (14.6–29.3)	14.6 (13.4–19.5)	22.9 (19.0–43.8)§
RV mass/volume ratio	0.32 (0.22–0.35)	0.23 (0.20–0.33)	0.34 (0.28–0.46)‖
LV ejection fraction, %	60±15	61±19	59±12
LV stroke volume index, mL/m^2	38±10	42±11	35±7
LV end-diastolic volume index, mL/m^2	68±24	75±29	61±18
LV mass index, g/m^2	57±18	58±19	55±18
RV-PA coupling			
Ees/Ea ratio	1.6±0.9	2.0±0.9	1.2±0.5†
Ees, mm Hg/mL	0.82±0.44	0.76±0.42	0.86±0.47
Ea, mm Hg/mL	0.59±0.37	0.38±0.05	0.80±0.43*

Values are mean±SD or median (interquartile range). CMR indicates cardiac magnetic resonance; Ea, arterial elastance; Ees, RV end-systolic elastance; LV, left ventricular; PA, pulmonary artery; PCWP, pulmonary capillary wedge pressure; PVR, pulmonary vascular resistance; RV, right ventricular; SVR, systemic vascular resistance; WU, Wood unit.
*P<0.01, †P<0.05, ‡P<0.001 (by t test) and §P<0.01, ‖P<0.05 (by Mann-Whitney test) for low PVR vs elevated PVR groups.

VTF as a Surrogate of Invasive Impedance

VTF is a surrogate of invasive impedance and not an exact measure of invasive impedance. Invasive impedance is the ratio of moduli of pressure by flow in frequency domain, whereas VTF is the ratio of moduli of output velocity profile/input velocity profile in frequency domain. As shown in Figure 2B for group with low PVR (<2.5 WUs), normal impedance curve shows a low modulus at 0 harmonic that rapidly descends down with first minimum achieved at low-frequency harmonics (harmonic 1 or 2). In contrast, the impedance modulus curve of the group with elevated PVR shows a high modulus at 0 harmonic, with delayed descent such that first minimum is not achieved at low-frequency harmonics and tends to occur at later harmonics (Figure 2B). This is the expected behavior of impedance curves,[4,5] and similar behavior in this study further lends support to the accuracy of impedance measurements in this study.

Corresponding VTF curves demonstrate that VTF curves start at similar moduli at 0 harmonic for subjects with normal or high PVR but then show differentiation at higher harmonics (5–7) when impedance moduli increase in subjects with high PVR (Figure 2A). For invasive impedance, the mean values of pressure and flow profiles are different, and thus their ratio leads to high impedance moduli at 0 and lower impedance harmonics. In contrast, for VTF, the input and output velocity curves in the PA have similar mean value, such that the VTF moduli at 0 and lower harmonics are close to 1 before separating at higher harmonics.

Interestingly, the MHFM of VTF were found to be increased in 2 patients with moderate elevation of PVR (2.5–3 WUs) and yet normal resting mean PA pressure (Figure 1). These 2

Table 3. PA Stiffness Parameters

Variables	All (n=20)	Low PVR (<2.5 WUs) (n=10)	High PVR (≥2.5 WUs) (n=10)
Completely noninvasive measures (CMR imaging only)			
MHFM of VTF	0.99 (0.86–1.48)	0.86 (0.57–0.96)	1.48 (1.03–2.93)*
Pulmonary/aortic diameter ratio	0.94±0.2	0.87±0.2	1.00±0.2
Pulsatility, %	19.4 (13.8–23.1)	20.1 (15.7–42.7)	18.7 (10.9–22.4)
Invasive measures (require both noninvasive imaging of PA and RHC)			
MLFM of impedance, mm Hg/L per min	2.48 (1.80–4.80)	1.80 (1.51–2.39)	4.80 (2.54–6.91)*
Compliance, mm^2/mm Hg	5.9±3.4	7.7±3.5	4.2±2.2†
Capacitance, cm^3/mm Hg	3.5±2.1	4.7±1.9	2.3±1.4‡
Distensibility, %/mm Hg	0.74 (0.44–1.24)	1.07 (0.76–2.34)	0.44 (0.36–0.69)*
Elastic modulus, mm Hg	156±94	94.5±54	217±84‡
Stiffness index	5.8±3.9	4.9±2.6	6.8±4.7

Values are mean±SD or median (interquartile range). CMR indicates cardiac magnetic resonance; MHFM, mean high-frequency modulus; MLFM, mean low-frequency modulus; PA, pulmonary artery; PVR, pulmonary vascular resistance; RHC, right-sided heart catheterization; VTF, velocity transfer function; WU, Wood unit.
*P<0.001 (by Mann-Whitney test) and †P<0.05, ‡P<0.01 (by t-test) and for low PVR vs elevated PVR groups.

subjects had interstitial lung disease. These patients also had relatively normal RVMI (19 and 21 g/m^2) and RV end-diastolic volume index (42 and 75 mL/m^2) but lower values of RV ejection fraction (44% and 29%) and Ees/Ea ratio (0.57 and 0.92). Further longitudinal studies of RV-PA coupling are needed to be better understand the temporality and magnitude of changes in VTF moduli with RV remodeling.

Advantages of VTF Over Current Methods for Assessing PA Stiffness

The role of CMR in the diagnosis and management of patients with PAH has increased in the recent years.[27,28] Most parameters of PA stiffness, including PA compliance, distensibility, capacitance, elasticity, and stiffness index, require a combined approach of invasive measurement of intrapulmonary pressures with RHC and noninvasive measurement of change in PA diameter or cross-sectional area within cardiac cycle.[28] The completely noninvasive measures of PA stiffness include comparison of PA diameter with aortic diameter and pulsatility, which is a measure of relative area change of PA within cardiac cycle without considering the distending PA pressures. However, these completely noninvasive measures were not significantly different in patients with low or high PVR in our study (Table 3).

PWV has been studied as a noninvasive measure of PA stiffness.[8,29–31] A major difficulty in measuring PWV is related to the change in the shape of pressure and flow waves with distance that makes it difficult to assign a single value that is definitive for the entire wave. In addition, PWV is affected by hemodynamic conditions at the time of measurement. Application of PWV to PA is further complicated by PA

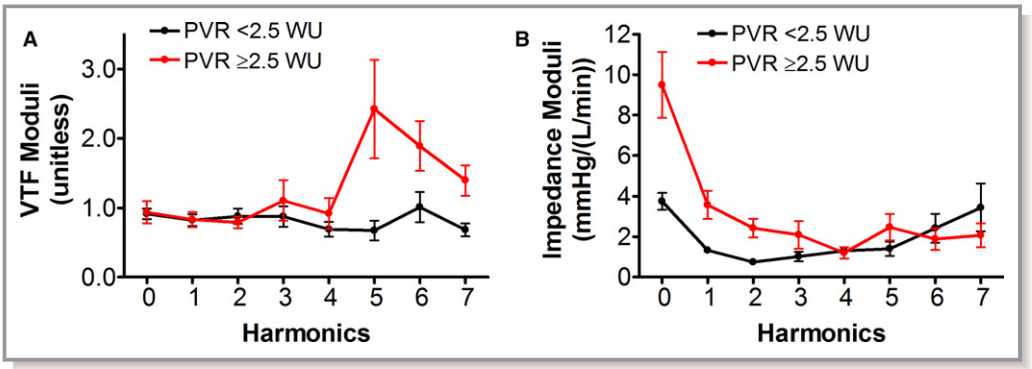

Figure 2. The velocity transfer function (VTF) and impedance curves. VTF (A) and invasive impedance (B) curves averaged for subjects with low pulmonary vascular resistance (PVR; <2.5 Wood units [WUs]; black), and subjects with high PVR (≥2.5 WUs; red).

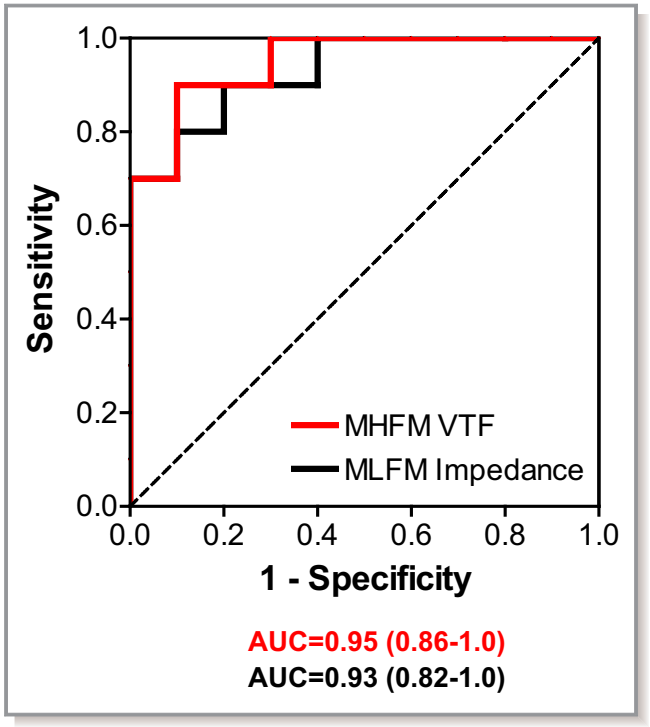

Figure 3. Receiver operating characteristic curves for discrimination of low vs high pulmonary vascular resistance (PVR). Mean high-frequency modulus (MHFM) of velocity transfer function (VTF; red) and mean low-frequency modulus (MLFM) of invasive impedance (black) showed similarly strong discrimination characteristics for low vs high PVR (≥2.5 Wood units). The 95% confidence interval of area under the curve (AUC) is shown in parentheses.

anatomical features because of its short distance and curvature, and a need for a high temporal resolution CMR.[32] Except studies measuring PWV in normal subjects,[30,31] other studies involving PWV and analysis of RV CMR indexes were performed in patients with advanced PAH with overall much higher values of mean pulmonary artery pressure and PVR, thus limiting its clinical use.[8,29,33,34] The latter is also true for studies applying the dynamic contrast–enhanced magnetic resonance imaging in pulmonary vascular system in patients with advanced PAH.[35,36] Further studies are required to evaluate the applicability and accuracy of these promising approaches in clinical use, especially in subjects with mildly elevated PVR, with mean PA pressure and PVR values close to the diagnostic thresholds for PAH[37] (as it was true for a substantial portion of the cohort in the present work).

VTF offers several advantages as a measure of PA stiffness. First, VTF can be reliably and accurately measured in a completely noninvasive manner. Second, VTF offers high sensitivity and specificity for detection of increased PA stiffness. This may have implications for noninvasive screening of patients for PAH, such as in patients with chronic obstructive pulmonary disease or in patients with rheumatic conditions, such as rheumatoid arthritis or scleroderma, that are associated with PAH. Third, VTF being in frequency domain is poised to be independent of hemodynamic conditions within physiologic ranges at the time of measurement, as detailed in rationale for VTF in data supplement. This may allow for comparisons between subjects or within same subject over time to be made independent of the individual heart rates and absolute systemic or pulmonary pressures. This requires validation in future longitudinal studies. Fourth, VTF can be rapidly acquired. The phase-contrast sequence to obtain VTF takes ≈10 minutes with fast postprocessing, which is fully automated with manual oversight. In addition, CMR imaging for VTF does not require intravenous contrast and, hence, patients do not need intravenous access. Fifth, simultaneous CMR assessment of right and left ventricular structure and function can be done, if clinically indicated, such as in patients with known or suspected PAH. This adds an additional 15 minutes of scan time for a total scan time for

Table 4. Association of VTF With RV Remodeling and RV-PA Coupling

	Spearman's Rank Correlation for MHFM of VTF With Parameters of RV Remodeling and RV-PA Coupling		
Parameter	ρ	95% CI	*P* Value
RV ejection fraction, %	−0.73	−0.89 to −0.40	<0.001
RV stroke volume index, mL/m^2	−0.20	−0.61 to 0.29	0.4
RV end-diastolic volume index, mL/m^2	0.34	−0.15 to 0.69	0.2
RV mass index, g/m^2	0.51	0.06 to 0.79	0.02
RV mass/volume ratio	0.42	−0.05 to 0.74	0.07
Ees/Ea ratio	−0.83	−0.93 to −0.59	<0.001
Ees, mm Hg/mL	−0.42	−0.74 to 0.06	0.08
Ea, mm Hg/mL	0.60	0.21 to 0.83	<0.01

CI indicates confidence interval; Ea, arterial elastance; Ees, RV end-systolic elastance; MHFH, mean high-frequency modulus; PA, pulmonary artery; RV, right ventricular; VTF, velocity transfer function.

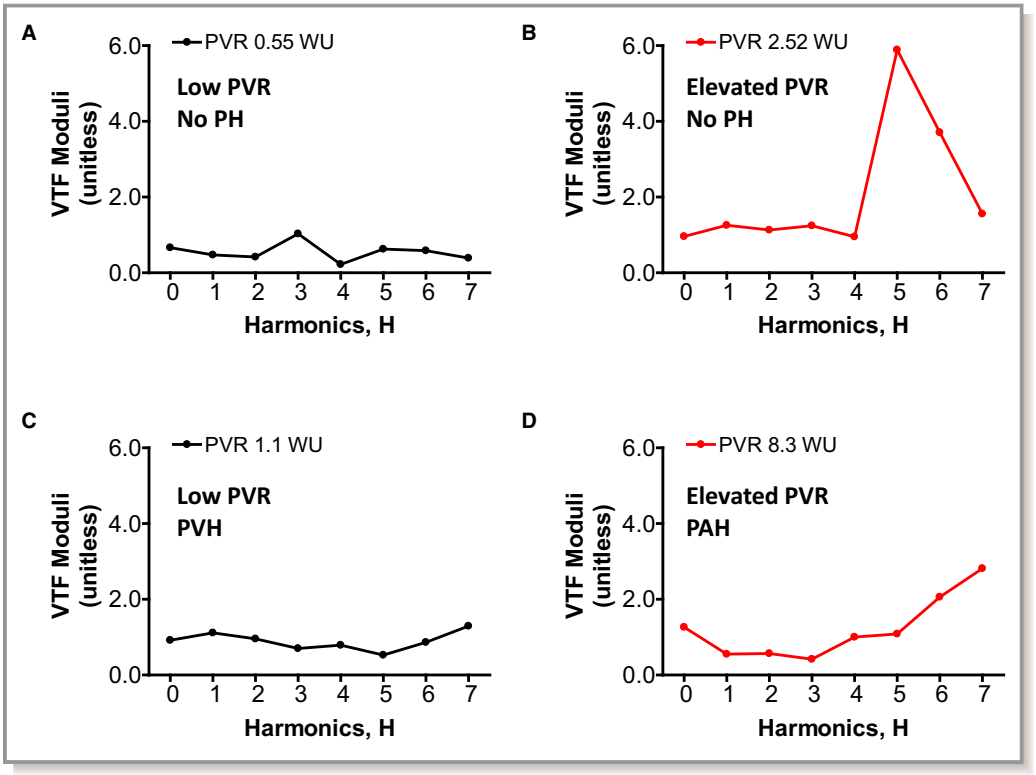

Figure 4. Individual subject examples of velocity transfer function (VTF) moduli curves. A, Subject with recurrent idiopathic syncope with otherwise no clinical pulmonary hypertension (PH), mean pulmonary artery pressure (mPAP) of 16 mm Hg, pulmonary capillary wedge pressure (PCWP) of 14 mm Hg, cardiac output (CO) of 5.4 L/min, and pulmonary vascular resistance (PVR) of 0.55 Wood units (WUs; normal). B, Subject with idiopathic pulmonary fibrosis with otherwise no clinical resting PH (mPAP of 19 mm Hg), PCWP of 5 mm Hg, CO of 5.5 L/min, and PVR of 2.52 WUs (moderate PVR elevation with yet normal mPAP). C, Subject with heart failure with preserved ejection fraction with elevated pulmonary pressures (mPAP of 30 mm Hg) secondary to elevated PCWP of 20 mm Hg, CO of 10.0 L/min, and PVR of 1.1 WUs (pulmonary venous hypertension [PVH]). D, Subject with idiopathic sporadic elevated pulmonary pressures (mPAP of 48 mm Hg), normal PCWP of 7 mm Hg, CO of 3.7 L/min, and elevated PVR of 8.3 WUs (pulmonary arterial hypertension [PAH]).

VTF and RV assessment under 30 minutes. This may aid in rapid clinical work flow, especially in busy PAH or heart failure clinics.

Limitations

There are several limitations in the present work. In this study, PA impedance was measured by using hybrid acquisition of pressure data from RHC and flow data from Doppler echocardiography. Although completely invasive assessment of PA impedance is feasible and was used in older studies in animals,[3,38,39] and humans,[6,40,41] most recent human studies on PA impedance have used the hybrid acquisition because of practicality and relative low expense.[9,12] To avoid errors attributable to hybrid acquisition of impedance, we obtained RHC and echocardiographic Doppler measurements either simultaneously or immediately next to each other, resulting in mean time difference between PA pressure and flow measurement of 0.03 hours. Another limitation is the use of fluid-filled catheter for acquisition of invasive PA pressure measurements during RHC, as opposed to use of high-fidelity catheters, which are not available for routine clinical practice and are expensive to use. However, the behavior of impedance curves in our study for patients with low versus high PVR was as expected and as previously described in literature, lending support to the accuracy of impedance measurements in our study.

The other limitation of this study is nonsimultaneous acquisition of invasive impedance (RHC-Doppler) and VTF (CMR). There are few hybrid CMR-RHC suites in the world. Thus, for all practical purposes, the only way currently to acquire RHC and CMR data in a patient is sequential. In this study, to minimize hemodynamic alterations between RHC and CMR acquisition, all studies in a participant were obtained on the same day as close to each other as logistically feasible, with a mean time difference between RHC and CMR of

2.4 hours. Although there was a close intraclass agreement of hemodynamic parameters of heart rate, blood pressure, and cardiac index at time of RHC and CMR (Table S1), the linear correlation between some of these parameters was moderate (Table S1). However, both VTF and impedance analyses are in frequency domain, rather than time domain; therefore, it is unlikely that the differences in hemodynamic parameters in physiologic range during RHC and CMR will adversely affect the VTF and impedance measurements. In this study, we measured VTF in the right PA and the impedance in the main PA. Therefore, if there may be heterogeneity in vessel stiffness in the pulmonary vasculature, such that much of the stiffness manifests in the main PA but not in the PA, the latter would be missed by this technique. Further research is needed to involve main PA in assessment of stiffness in pulmonary vasculature using VTF technique. The current study includes a small, but well-characterized, cohort with prospective enrollment and acquisition of impedance and VTF data. Therefore, a larger study is warranted for further evaluation of this novel noninvasive method for assessment of PA stiffness. In addition, all our study participants by inclusion criteria were adults aged >18 years. Applicability of VTF in children in whom noninvasive assessment of PAH could be even more beneficial is unknown and needs investigation.

In conclusion, we have introduced a novel noninvasive parameter, VTF, that could reliably be used as a surrogate estimate of PA impedance and detection of PA stiffness using CMR. Further large and longitudinal studies are needed to evaluate the diagnostic accuracy of VTF as a screening tool for the assessment of increased PVR and for serial assessment of changes in PVR with therapy.

Sources of Funding

This work was supported by the Walter B. Frommeyer, Jr, Fellowship in Investigative Medicine (A. Gupta) from the Department of Medicine at the University of Alabama at Birmingham (Birmingham, AL).

Disclosures

The University of Alabama at Birmingham and Auburn University co-own the patent (H. Gupta, T.S. Denney, and A. Gupta are coinventors). Arcus-Med, LLC, has the exclusive rights. H. Gupta and T.S. Denney are major stakeholders in Arcus-Med, LLC. The remaining authors have no disclosures to report.

References

1. McLaughlin VV, Archer SL, Badesch DB, Barst RJ, Farber HW, Lindner JR, Mathier MA, McGoon MD, Park MH, Rosenson RS, Rubin LJ, Tapson VF, Varga J, Harrington RA, Anderson JL, Bates ER, Bridges CR, Eisenberg MJ, Ferrari VA, Grines CL, Hlatky MA, Jacobs AK, Kaul S, Lichtenberg RC, Lindner JR, Moliterno DJ, Mukherjee D, Pohost GM, Rosenson RS, Schofield RS, Shubrooks SJ, Stein JH, Tracy CM, Weitz HH, Wesley DJ. ACCF/AHA 2009 expert consensus document on pulmonary hypertension: a report of the American College of Cardiology Foundation Task Force on expert consensus documents and the American Heart Association: developed in collaboration with the American College of Chest Physicians, American Thoracic Society, Inc., and the Pulmonary Hypertension Association. *Circulation*. 2009;119:2250–2294.
2. Bertand ME, Widimsky J. Vascular resistance. *Eur Heart J*. 1985;6(suppl C):19.
3. Milnor WR, Bergel DH, Bargainer JD. Hydraulic power associated with pulmonary blood flow and its relation to heart rate. *Circ Res*. 1966;19:467–480.
4. O'Rourke MF. Vascular impedance in studies of arterial and cardiac function. *Physiol Rev*. 1982;62:570–623.
5. Piene H. Pulmonary arterial impedance and right ventricular function. *Physiol Rev*. 1986;66:606–652.
6. Milnor WR, Conti CR, Lewis KB, O'Rourke MF. Pulmonary arterial pulse wave velocity and impedance in man. *Circ Res*. 1969;25:637–649.
7. Dell'Italia LJ, Santamore WP. Can indices of left ventricular function be applied to the right ventricle? *Prog Cardiovasc Dis*. 1998;40:309–324.
8. Sanz J, Kariisa M, Dellegrottaglie S, Prat-Gonzalez S, Garcia MJ, Fuster V, Rajagopalan S. Evaluation of pulmonary artery stiffness in pulmonary hypertension with cardiac magnetic resonance. *JACC Cardiovasc Imaging*. 2009;2:286–295.
9. Huez S, Brimioulle S, Naeije R, Vachiery JL. Feasibility of routine pulmonary arterial impedance measurements in pulmonary hypertension. *Chest*. 2004;125:2121–2128.
10. Kovacs G, Olschewski A, Berghold A, Olschewski H. Pulmonary vascular resistances during exercise in normal subjects: a systematic review. *Eur Respir J*. 2012;39:319–328.
11. Butler J, Chomsky DB, Wilson JR. Pulmonary hypertension and exercise intolerance in patients with heart failure. *J Am Coll Cardiol*. 1999;34:1802–1806.
12. Hunter KS, Lee PF, Lanning CJ, Ivy DD, Kirby KS, Claussen LR, Chan KC, Shandas R. Pulmonary vascular input impedance is a combined measure of pulmonary vascular resistance and stiffness and predicts clinical outcomes better than pulmonary vascular resistance alone in pediatric patients with pulmonary hypertension. *Am Heart J*. 2008;155:166–174.
13. Kramer CM, Barkhausen J, Flamm SD, Kim RJ, Nagel E. Standardized cardiovascular magnetic resonance (CMR) protocols 2013 update. *J Cardiovasc Magn Reson*. 2013;15:91.
14. Fratz S, Chung T, Greil GF, Samyn MM, Taylor AM, Valsangiacomo Buechel ER, Yoo SJ, Powell AJ. Guidelines and protocols for cardiovascular magnetic resonance in children and adults with congenital heart disease: SCMR expert consensus group on congenital heart disease. *J Cardiovasc Magn Reson*. 2013;15:51.
15. Feng W, Nagaraj H, Gupta H, Lloyd SG, Aban I, Perry GJ, Calhoun DA, Dell'Italia LJ, Denney TS Jr. A dual propagation contours technique for semi-automated assessment of systolic and diastolic cardiac function by CMR. *J Cardiovasc Magn Reson*. 2009;11:30.
16. Wells JM, Iyer AS, Rahaghi FN, Bhatt SP, Gupta H, Denney TS, Lloyd SG, Dell'Italia LJ, Nath H, Estepar RS, Washko GR, Dransfield MT. Pulmonary artery enlargement is associated with right ventricular dysfunction and loss of blood volume in small pulmonary vessels in chronic obstructive pulmonary disease. *Circ Cardiovasc Imaging*. 2015;8:e002546.
17. Brewis MJ, Bellofiore A, Vanderpool RR, Chesler NC, Johnson MK, Naeije R, Peacock AJ. Imaging right ventricular function to predict outcome in pulmonary arterial hypertension. *Int J Cardiol*. 2016;218:206–211.
18. Vanderpool RR, Pinsky MR, Naeije R, Deible C, Kosaraju V, Bunner C, Mathier MA, Lacomis J, Champion HC, Simon MA. RV-pulmonary arterial coupling predicts outcome in patients referred for pulmonary hypertension. *Heart*. 2015;101:37–43.
19. Sanz J, Garcia-Alvarez A, Fernandez-Friera L, Nair A, Mirelis JG, Sawit ST, Pinney S, Fuster V. Right ventriculo-arterial coupling in pulmonary hypertension: a magnetic resonance study. *Heart*. 2012;98:238–243.
20. Kelly RP, Ting CT, Yang TM, Liu CP, Maughan WL, Chang MS, Kass DA. Effective arterial elastance as index of arterial vascular load in humans. *Circulation*. 1992;86:513–521.
21. Schwartzenberg S, Redfield MM, From AM, Sorajja P, Nishimura RA, Borlaug BA. Effects of vasodilation in heart failure with preserved or reduced ejection fraction implications of distinct pathophysiologies on response to therapy. *J Am Coll Cardiol*. 2012;59:442–451.

22. Hankinson SE, Manson JE, Spiegelman D, Willett WC, Longcope C, Speizer FE. Reproducibility of plasma hormone levels in postmenopausal women over a 2-3-year period. *Cancer Epidemiol Biomarkers Prev*. 1995;4:649–654.
23. Gilbert-Kawai E, Wittenberg M. Pulmonary vascular resistance. In: Gilbert-Kawai E, Wittenberg M, eds. *Essential Equations for Anaesthesia: Key Clinical Concepts for the FRCA and EDA*. Cambridge: Cambridge University Press; 2014:134–135.
24. Maron BA, Loscalzo J. Pulmonary hypertension in non-pulmonary arterial hypertension patients. In: Creager MA, Beckman JA, Loscalzo J, eds. *Vascular Medicine: A Companion to Braunwald's Heart Disease*. Philadelphia, PA: Elsevier; 2013:687–696.
25. Hoeper MM, Bogaard HJ, Condliffe R, Frantz R, Khanna D, Kurzyna M, Langleben D, Manes A, Satoh T, Torres F, Wilkins MR, Badesch DB. Definitions and diagnosis of pulmonary hypertension. *J Am Coll Cardiol*. 2013;62:D42–D50.
26. Chang PP, Longenecker JC, Wang NY, Baughman KL, Conte JV, Hare JM, Kasper EK. Mild vs severe pulmonary hypertension before heart transplantation: different effects on posttransplantation pulmonary hypertension and mortality. *J Heart Lung Transplant*. 2005;24:998–1007.
27. Benza R, Biederman R, Murali S, Gupta H. Role of cardiac magnetic resonance imaging in the management of patients with pulmonary arterial hypertension. *J Am Coll Cardiol*. 2008;52:1683–1692.
28. Freed BH, Collins JD, Francois CJ, Barker AJ, Cuttica MJ, Chesler NC, Markl M, Shah SJ. MR and CT imaging for the evaluation of pulmonary hypertension. *JACC Cardiovasc Imaging*. 2016;9:715–732.
29. Gan CT, Lankhaar JW, Westerhof N, Marcus JT, Becker A, Twisk JW, Boonstra A, Postmus PE, Vonk-Noordegraaf A. Noninvasively assessed pulmonary artery stiffness predicts mortality in pulmonary arterial hypertension. *Chest*. 2007;132:1906–1912.
30. Forouzan O, Warczytowa J, Wieben O, Francois CJ, Chesler NC. Non-invasive measurement using cardiovascular magnetic resonance of changes in pulmonary artery stiffness with exercise. *J Cardiovasc Magn Reson*. 2015;17:109.
31. Bradlow WM, Gatehouse PD, Hughes RL, O'Brien AB, Gibbs JS, Firmin DN, Mohiaddin RH. Assessing normal pulse wave velocity in the proximal pulmonary arteries using transit time: a feasibility, repeatability, and observer reproducibility study by cardiovascular magnetic resonance. *J Magn Reson Imaging*. 2007;25:974–981.
32. Ibrahim el SH, Shaffer JM, White RD. Assessment of pulmonary artery stiffness using velocity-encoding magnetic resonance imaging: evaluation of techniques. *Magn Reson Imaging*. 2011;29:966–974.
33. Zhang Z, Wang M, Yang Z, Yang F, Li D, Yu T, Zhang N. Noninvasive prediction of pulmonary artery pressure and vascular resistance by using cardiac magnetic resonance indices. *Int J Cardiol*. 2017;227:915–922.
34. Swift AJ, Rajaram S, Hurdman J, Hill C, Davies C, Sproson TW, Morton AC, Capener D, Elliot C, Condliffe R, Wild JM, Kiely DG. Noninvasive estimation of PA pressure, flow, and resistance with CMR imaging: derivation and prospective validation study from the ASPIRE registry. *JACC Cardiovasc Imaging*. 2013;6:1036–1047.
35. Swift AJ, Telfer A, Rajaram S, Condliffe R, Marshall H, Capener D, Hurdman J, Elliot C, Kiely DG, Wild JM. Dynamic contrast-enhanced magnetic resonance imaging in patients with pulmonary arterial hypertension. *Pulm Circ*. 2014;4:61–70.
36. Skrok J, Shehata ML, Mathai S, Girgis RE, Zaiman A, Mudd JO, Boyce D, Lechtzin N, Lima JA, Bluemke DA, Hassoun PM, Vogel-Claussen J. Pulmonary arterial hypertension: MR imaging-derived first-pass bolus kinetic parameters are biomarkers for pulmonary hemodynamics, cardiac function, and ventricular remodeling. *Radiology*. 2012;263:678–687.
37. Galie N, Humbert M, Vachiery JL, Gibbs S, Lang I, Torbicki A, Simonneau G, Peacock A, Vonk Noordegraaf A, Beghetti M, Ghofrani A, Gomez Sanchez MA, Hansmann G, Klepetko W, Lancellotti P, Matucci M, McDonagh T, Pierard LA, Trindade PT, Zompatori M, Hoeper M, Aboyans V, Vaz Carneiro A, Achenbach S, Agewall S, Allanore Y, Asteggiano R, Paolo Badano L, Albert Barbera J, Bouvaist H, Bueno H, Byrne RA, Carerj S, Castro G, Erol C, Falk V, Funck-Brentano C, Gorenflo M, Granton J, Iung B, Kiely DG, Kirchhof P, Kjellstrom B, Landmesser U, Lekakis J, Lionis C, Lip GY, Orfanos SE, Park MH, Piepoli MF, Ponikowski P, Revel MP, Rigau D, Rosenkranz S, Voller H, Luis Zamorano J. 2015 ESC/ERS guidelines for the diagnosis and treatment of pulmonary hypertension: the Joint Task Force for the diagnosis and treatment of pulmonary hypertension of the European Society of Cardiology (ESC) and the European Respiratory Society (ERS): endorsed by: Association for European Paediatric and Congenital Cardiology (AEPC), International Society for Heart and Lung Transplantation (ISHLT). *Eur Heart J*. 2016;37:67–119.
38. Caro CG, McDonald DA. The relation of pulsatile pressure and flow in the pulmonary vascular bed. *J Physiol*. 1961;157:426–453.
39. Bergel DH, Milnor WR. Pulmonary vascular impedance in the dog. *Circ Res*. 1965;16:401–415.
40. Murgo JP, Westerhof N. Input impedance of the pulmonary arterial system in normal man: effects of respiration and comparison to systemic impedance. *Circ Res*. 1984;54:666–673.
41. Chen YT, Chen KS, Chen JS, Lin WW, Hu WH, Chang MK, Lee DY, Lee YS, Lin JR, Chiang BN. Aortic and pulmonary input impedance in patients with cor pulmonale. *Jpn Heart J*. 1990;31:619–629.

Supplemental Material

Data S1. Rationale For Velocity Transfer Function

Pulmonary Arterial (PA) Impedance

In the PA system, impedance describes the frequency dependent relationship between pressure and flow.[1] Impedance takes into account the pulsatile nature of blood flow. The compliance or stiffness of the PA and the resistance from blood viscosity and the distal capillary bed determine the frequency-dependent manner in which pressure and flow are related. Figure S1 shows pressure and flow curves measured in a patient with PA hypertension (PAH). If the pressure and flow are measured at a point, the resulting impedance is called input impedance or simply impedance. Input impedance is relatively easy to measure and calculate, but it is affected by reflected waves in both the pressure and flow curves.[2, 3] If the reflected waves are removed through post-processing techniques, the result is called characteristic impedance.[2, 3] In this paper, we exclusively use input impedance, and the term impedance refers to input impedance. Time-varying pressure and flow can be decomposed into frequency components using Fourier analysis. The PA impedance describes how each frequency component in the flow is related to its counterpart in the pressure in terms of magnitude and phase. The impedance magnitude describes how each frequency component is amplified (magnitude>1) or attenuated (magnitude<1) in the vessel. At a frequency of zero Hertz, the impedance describes the relationship between mean PA pressure and mean PA flow and its modulus is approximately equal to pulmonary vascular resistance. With normal arterial stiffness, the zero frequency modulus is low, as would be expected, followed by a rapid decline in impedance modulus with first minimum occurring at first or second harmonic. With increased arterial stiffness, the zero frequency modulus increase, there is decreased rate of decline of modulus with corresponding increase in frequency when the first minimum of modulus occurs.[1] As a result, in animal studies under serotonin or induced hypoxia which increases vascular resistance and PA stiffness, impedance moduli are larger than controls.[1] Similar results have been shown in humans where impedance moduli in patients with PAH are larger than in controls.[4]

Velocity Transfer Function

PA pressure measurements are obtained by invasive techniques for quantification of PA impedance. Velocity and flow, however, can be measured non-invasively with phase-contrast cardiac magnetic resonance (CMR) at arbitrary points in the PA tree. Figure S2 shows the examples of pulsatile velocity profiles measured at the proximal point of PA (input velocity profile) and the distal point of PA (output velocity profile) in a normal human volunteer and a patient with PAH. In a normal volunteer, with a compliant PA, the velocity profile not only is shifted in the transit time between the two sites, but there are also complex shape changes across the entire wave. In a patient with PAH, the PA is stiffer and both the time shift and shape change are reduced. These time shifts and shape changes are frequency dependent and are related to the compliance and geometry of the artery between the two points. These frequency-dependent changes can be compactly described by the transfer function between the two velocity profiles. A transfer function is a function that describes the relationship between the frequency spectra of any two functions that are linearly related. Impedance is a specific case of a transfer function when the two functions are voltage and current or pressure and flow. Here velocity transfer function (VTF [$S_F(f)$]) was computed between measured velocity profiles at the input and the output points of the PA by taking the Fourier transform of each velocity profile and dividing one by other as follows:

$$S_F\,(f) = V_{PA\text{-}distal}\,(f) \,/\, V_{PA\text{-}proximal}\,(f)$$

Ideally, in a stiff PA, with little change in shape of the velocity profile as it moves through a section of artery, the VTF is a relatively flat as shown in the right side of Figure S2. In a compliant PA, the VTF is reduced at higher frequencies. In actual MRI data, the VTF magnitude profiles may differ substantially from the ideal ones in Figure S2, but larger VTF magnitudes in the higher frequencies are associated with increased PA stiffness.

The VTF measured by this method is similar to impedance because it describes predominantly the influence of vessel geometry and compliance/stiffness to cause frequency-dependent changes in the input velocity profile as it travels through the artery thereby producing the output velocity profile. Similar to

impedance, VTF is affected by reflected waves, but the effect is small, as described below. Importantly, VTF can be measured non-invasively with phase contrast CMR. In the case of a stiff tube, the velocity wave profile will amplify and the high frequency modulus of VTF will be high. In contrast, if the PA is compliant the velocity wave will dampen and the high frequency modulus of VTF will be low.

Influence of Heart Rate and Pressure on Velocity Transfer Function

Expressing VTF in harmonics allows comparisons between subjects or in the same subject over time to be made independent of the individual heart rates. VTF inherently measures the behavior of a section of PA in response to pulsatile inputs driven by changing pressure gradients. Consequently, VTF is relatively insensitive to pressure over a wide range of absolute pressures.

Table S1. Inter-modality hemodynamic correlation and agreement.

Parameter	Correlation		Agreement	
	Pearson r	p-value	Relative bias	p-value
HR, bpm				
RHC-Doppler	0.81	<0.0001	4.15±4.92	0.68
RHC-MRI	0.75	0.0002	6.3±4.16	0.93
BP, mm Hg, RHC-CMR				
SBP	0.76	0.0002	11.83±9.94	0.67
DBP	0.49	0.04	11.89±9.8	0.46
MBP	0.65	0.004	10.5±9.02	0.49
CI, L/min/$m^{2,}$, RHC-CMR	0.69	0.0008	0.52±0.37	0.74

Inter-modality heart rate (HR), blood pressure (BP), and cardiac index (CI) differences are expressed as mean ± SD. CMR, cardiac magnetic resonance; DBP, diastolic blood pressure; MBP, mean blood pressure; RHC, right heart catheterization; SBP, systolic blood pressure.

Table S2. Pulmonary artery stiffness parameters measured in study.

Parameters	Definition	Formula	Units	Technique
Completely Non-Invasive				
Velocity Transfer Function (VTF)	Transfer function of velocity between proximal PA (input) and distal PA (output).	$V_{PA\text{-}distal}(f)/V_{PA\text{-}proximal}(f)$	unitless	CMR
PA-Aortic Diameter Ratio	Ratio of main PA to aortic root diameter	PA diameter/ Aortic root diameter	unitless	CMR
Pulsatility	Relative area change of main PA	[(maxA-minA)/minA] x 100	%	CMR
Require Invasive Measurements				
Impedance Modulus (Z)	Ratio of modulus of pressure and flow	|P|/|Q|	mm Hg/(L/min)	RHC + Doppler
PVR	Static resistance	$(P_2\text{-}P_1)/Q$	Woods Units	RHC
Capacitance	Volume change per unit pressure	SV/PP	cm^3/mm Hg	RHC
Compliance	Area change per unit pressure	(maxA-minA)/PP	mm^2/mm Hg	RHC + CMR
Distensibility	Relative area change per unit pressure	[(maxA-minA) /minA x PP] x 100	%/mm Hg	RHC + CMR
Elastic Modulus	Driving pressure effecting a unit relative area change	(PP x minA)/ (maxA-minA)	mm Hg	RHC + CMR
Stiffness Index	Slope of function between distending arterial pressure and arterial distention	[ln(PASP/PADP)]/[(maxA - minA)/minA]	unitless	RHC + CMR

A, area; CMR, cardiac magnetic resonance; PA, pulmonary artery; P, pressure; PASP, pulmonary artery systolic pressure; PADP, pulmonary artery diastolic pressure; PP, pulse pressure; Q, flow; RHC, right heart catheterization; V(f), velocity-time profile.

Table S3. Association of VTF with standard non-invasive/invasive parameters of pulmonary arterial stiffness.

Parameter	Spearman's rank correlation with MHFM of VTF		
	rho	95% CI	p-value
Pulmonary to aortic diameter ratio	0.19	-0.29, 0.59	0.4
Pulsatility, %	-0.47	-0.76, -0.02	0.04
Compliance, mm^2/mmHg	-0.52	-0.79, -0.09	0.02
Capacitance, cm^3/mmHg	-0.57	-0.82, -0.16	<0.01
Distensibility, %/mmHg	-0.55	-0.80, -0.12	0.01
Elastic modulus, mmHg	0.55	0.13, 0.80	0.01
Stiffness index	0.33	-0.15, 0.68	0.2

MHFM: mean high frequency modulus; MLFM: mean low frequency modulus; VTF: velocity transfer function.

Table S4. Intra- and inter-observer reliability in measurement of mean high frequency moduli of VTF.

Parameter	Correlation		Agreement	
	Intra-Class Correlation Coefficient	95% CI	Relative bias±SD (mean difference ± SD)	P-value (μ_0: Bias =0)
Intra-observer	0.93	0.84-0.97	0.19±0.54	0.13
Inter-observer	0.94	0.87-0.98	0.05±0.28	0.97

Figure S1. Mean PA pressure and flow curves (left) in a patient with pulmonary hypertension.

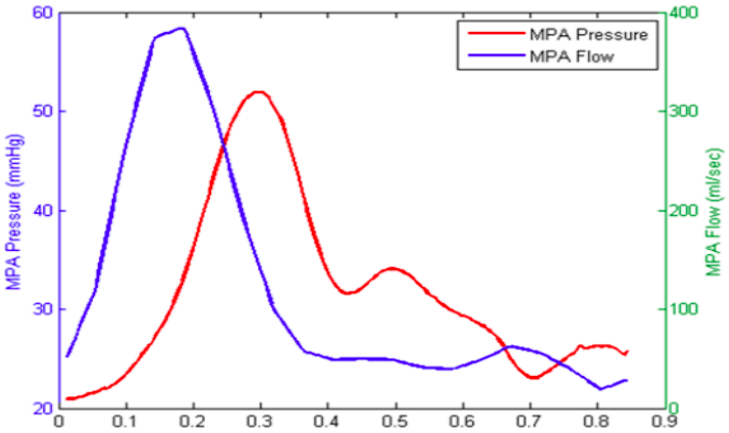

MPA: main pulmonary artery.

Figure S2. Examples of pulsatile velocity profiles measured at the proximal point of PA (input velocity profile) and the distal point of PA (output velocity profile) in a normal human volunteer and a patient with PAH.

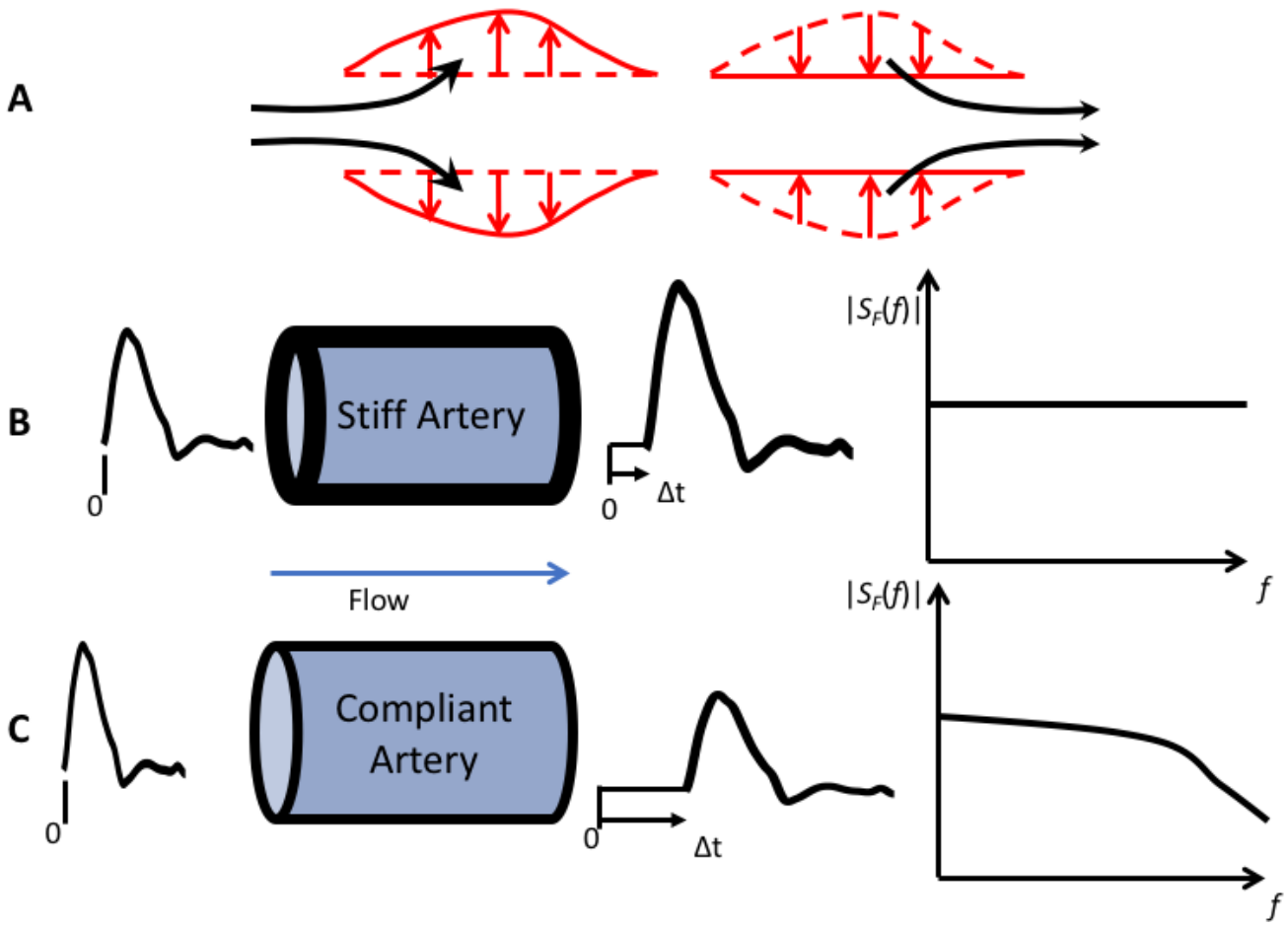

A: Flow into a PA causes distension of the vessel wall that recoils back to the original state, which results in the pulsatile component of PA impedance. In a stiff PA, the output waveform is a scaled and shifted version of the input waveform (B, left), which results in a transfer function with a constant modulus (B, right). In a compliant tube, the output of the tube has a more complex relationship with the input waveform (C, right). PA: pulmonary artery; PAH: pulmonary artery hypertension.

Figure S3. Digitization of pressure waveform and pulsed-wave Doppler waveform in the main pulmonary artery in one cardiac cycle

A. Digitization of pressure waveform in the main pulmonary artery in one cardiac cycle.

B. Digitization of pulsed wave Doppler waveform in the main pulmonary artery in one cardiac cycle.

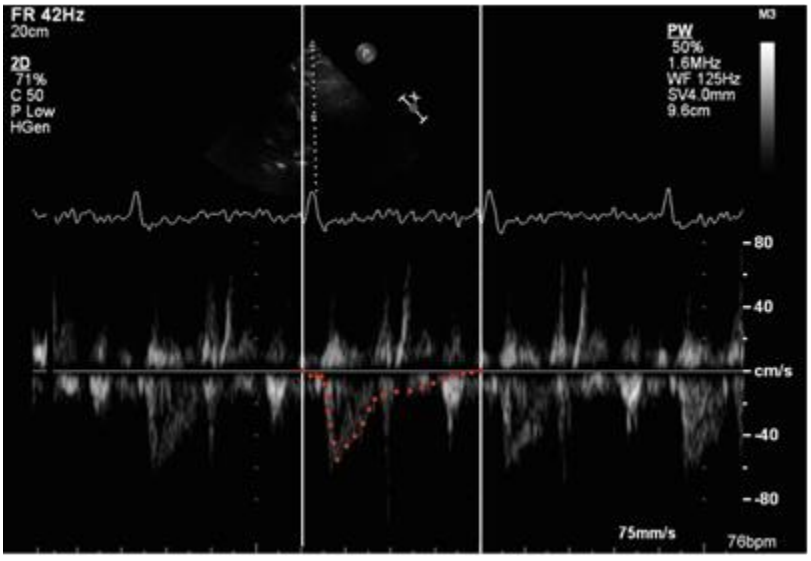

The digital data was extracted as comma separated values format for further analysis. The velocity profile was converted to flow profile as described in the Methods.

Figure S4. Acquisition of mean velocity profiles in proximal and distal portions of the right PA using phase-contrast CMR.

A. Phase-contrast CMR images

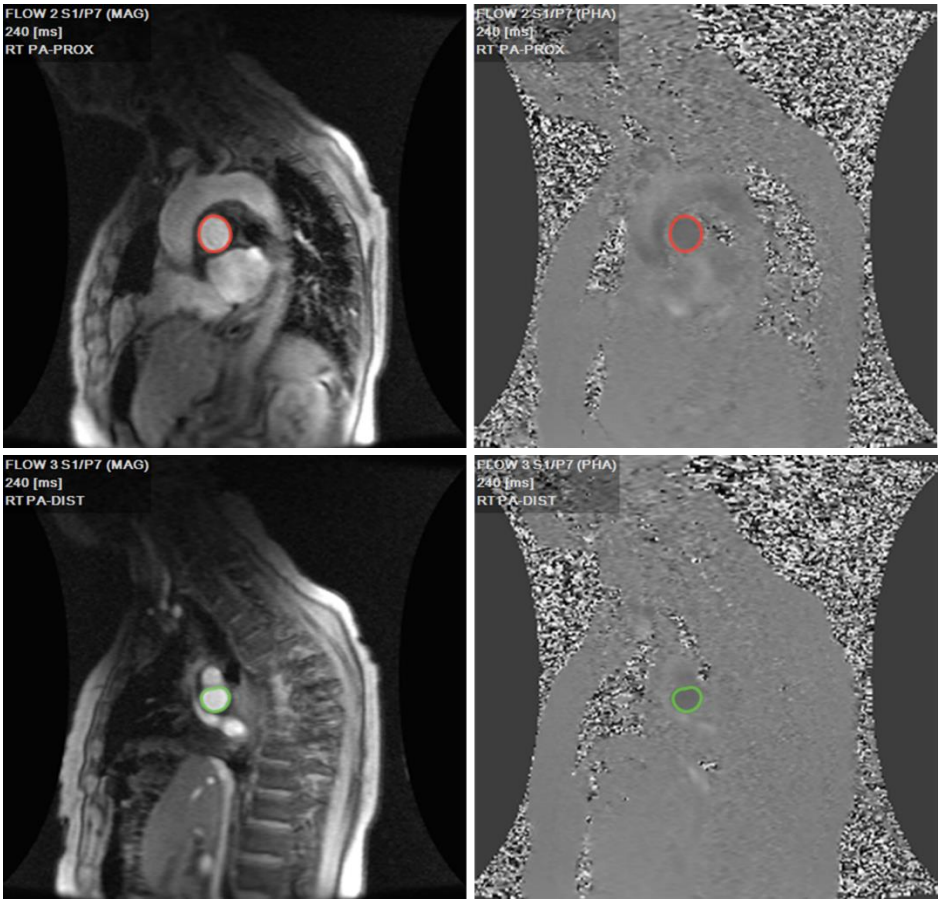

Representative images of phase-contrast CMR for the proximal (top) and distal (bottom) portions of right PA are shown. Semi-automated contouring of proximal (red) and distal (green) right PA with manual corrections as needed was performed using CAAS Flow 1.2 (Pie Medical Imaging, Netherland) analysis tools.

B. Mean velocity profiles over time for the proximal (red) and distal (green) portions of right PA

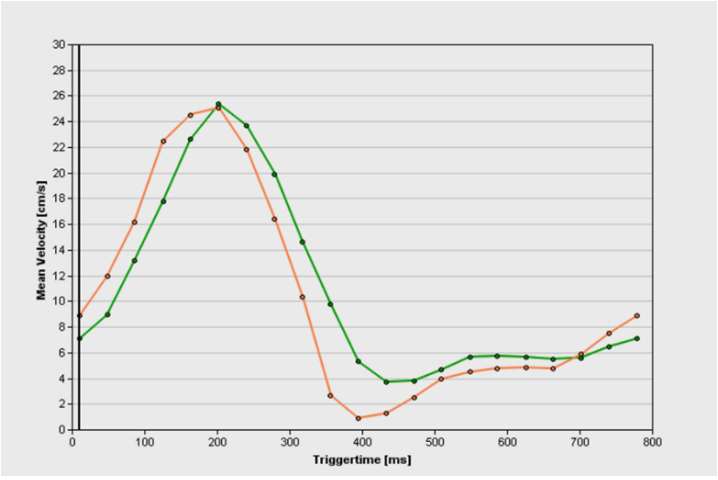

Figure S5. Scatterplot graphs depicting the relationships between mean high frequency moduli (MHFM) of velocity transfer function (VTF), mean low frequency moduli (MLFM) of impedance, and pulmonary vascular resistance (PVR).

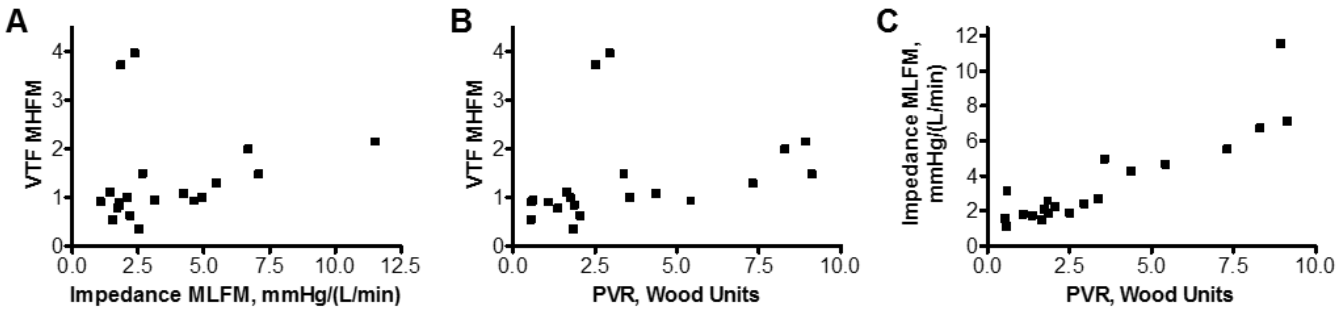

The strength of relationships was evaluated by Spearman's rank correlation coefficient (rho). A) Spearman's rho was 0.49, 95% CI: 0.41-0.77, p=0.03, for correlation between MHFM of VTF and MLFM of impedance. B) Spearman's rho was 0.63, 95% CI: 0.24-0.84, p=0.003, for correlation between MHFM of VTF and PVR. C) Spearman's rho was 0.86, 95% CI: 0.67-0.94, p<0.001, for correlation between MLFM of impedance and PVR.

Figure S6. Receiver operating characteristic (ROC) curves for mean high frequency moduli (MHFM) of velocity transfer function (VTF) to differentiate study subjects with elevated vs. normal pulmonary vascular resistance (PVR) at different thresholds of PVR.

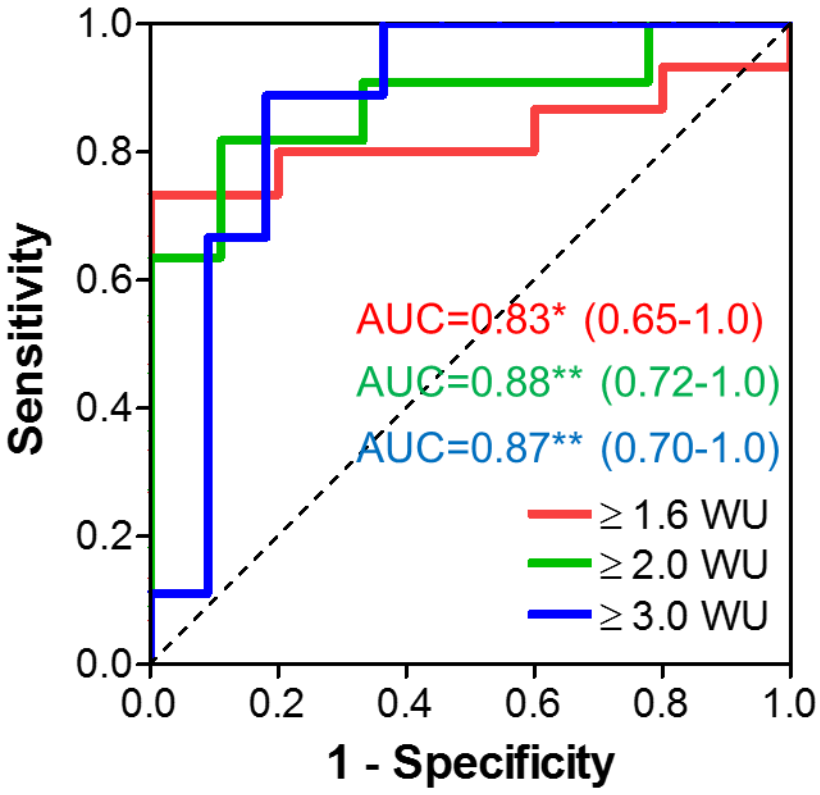

*P<0.05, **P<0.01. AUC: Area under curve; WU: Woods Units.

Figure S7. Scatterplot graphs depicting the relationships between mean high frequency moduli (MHFM) of velocity transfer function (VTF) and right ventricular (RV) structure, function, and RV-pulmonary artery (PA) coupling parameters.

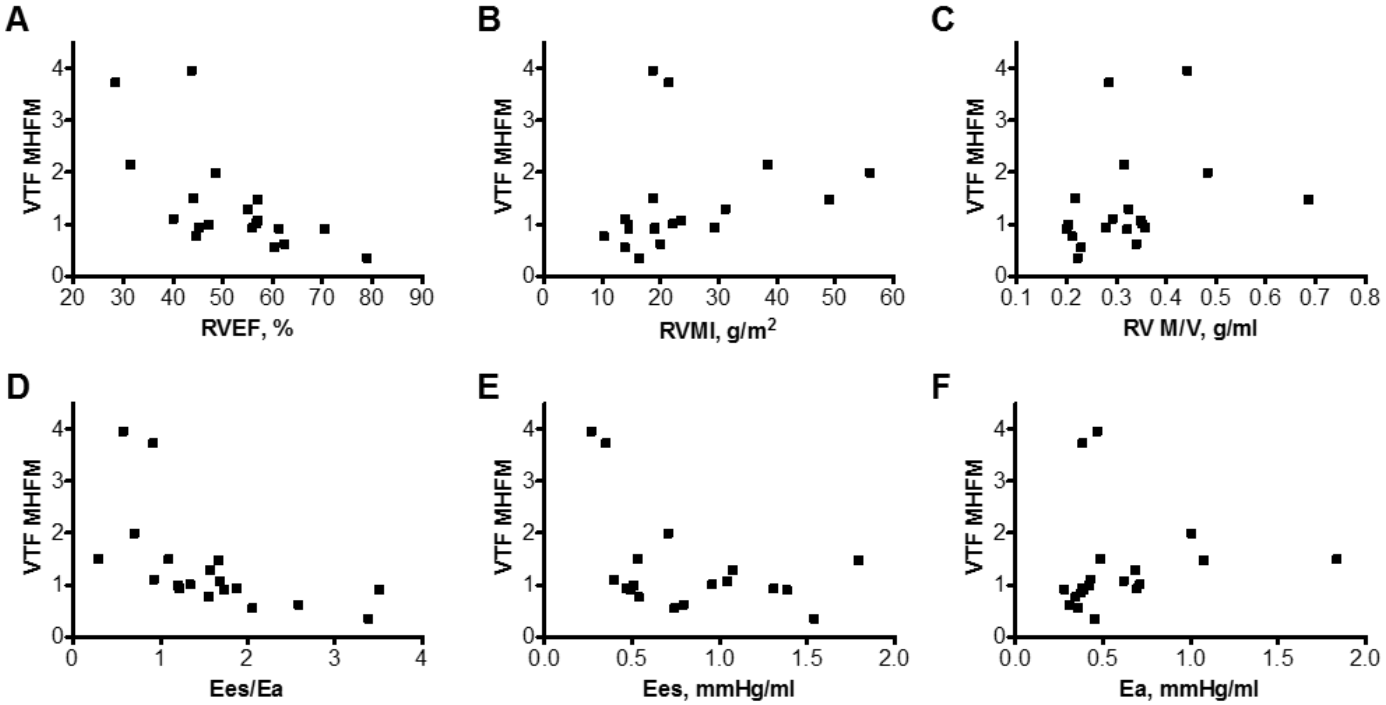

The strength of relationships was evaluated by Spearman's rank correlation coefficient (rho). A) Spearman's rho was -0.73, 95% CI: -0.89 - -0.40, p<0.001, for correlation between MHFM of VTF and RV ejection fraction (RVEF). B) Spearman's rho was 0.51, 95% CI: 0.06-0.79, p=0.003, for correlation between MHFM of VTF and RV mass index (RVMI). C) Spearman's rho was 0.42, 95% CI: -0.05-0.74, p<0.001, for correlation between MLFM of impedance and RV mass/volume ratio. D) Spearman's rho was -0.83, 95% CI: -0.93 - -0.59, p<0.001, for correlation between MHFM of VTF and RV end-systolic elastance (Ees)/pulmonary artery elastance (Ea) ratio. E) Spearman's rho was -0.42, 95% CI: -0.74 – 0.06, p=0.08, for correlation between MHFM of VTF and RV Ees. F) Spearman's rho was 0.60, 95% CI: 0.21 - 0.83, p<0.01, for correlation between MHFM of VTF and pulmonary artery Ea.

Supplemental References:

1. Piene H. Pulmonary arterial impedance and right ventricular function. *Physiological reviews*. 1986;66:606-52.
2. Murgo JP and Westerhof N. Input impedance of the pulmonary arterial system in normal man. Effects of respiration and comparison to systemic impedance. *Circulation research*. 1984;54:666-73.
3. Murgo JP, Westerhof N, Giolma JP and Altobelli SA. Aortic input impedance in normal man: relationship to pressure wave forms. *Circulation*. 1980;62:105-16.
4. Haneda T, Nakajima T, Shirato K, Onodera S and Takishima T. Effects of oxygen breathing on pulmonary vascular input impedance in patients with pulmonary hypertension. *Chest*. 1983;83:520-7.